*Response of the Japanese flying squid (*Todarodes pacificus*) in the Japan Sea to future climate warming scenarios*

Fei Ji, Xinyu Guo, Yucheng Wang & Katsumi Takayama

Climatic Change
An Interdisciplinary, International Journal Devoted to the Description, Causes and Implications of Climatic Change

ISSN 0165-0009

Climatic Change
DOI 10.1007/s10584-020-02689-3

Springer

Climatic Change
https://doi.org/10.1007/s10584-020-02689-3

Response of the Japanese flying squid (*Todarodes pacificus*) in the Japan Sea to future climate warming scenarios

Fei Ji[1,2] • **Xinyu Guo**[2] • **Yucheng Wang**[2,3] • **Katsumi Takayama**[4]

Received: 5 November 2019 / Accepted: 26 February 2020/

Abstract

The Japanese flying squid (*Todarodes pacificus*) is an important fishery resource in East Asia, including Japan, China, and Korea. Recent studies have suggested that it exhibits significant interannual variation with a close relationship with environmental variables, among which water temperature has an apparent influence on its spawning, hatching, and growth. Therefore, we need to understand how the Japanese flying squid in the Japan Sea (JS) will be affected by global warming. Based on particle tracking methods, we simulated migration and individual growth of Japanese flying squid from spawning to juveniles (182 days) in six cases: one for high-level catch years (1960–1966), one for low-level catch years (2008–2014), and four for the future, including two for 50 years (2056–2062) and two for 100 years from now (2104–2110) under the warming scenario of RCP2.6 and RCP8.5, respectively. The simulations showed that the number of squid increased with warming. The main reason for the increase was the warming of the JS, which increased the survival rate of autumn- and winter-spawning cohorts. In addition, the model also demonstrated the potential effects of warming on the physiological process of the early life stage of the Japanese flying squid.

Keywords Japanese flying squid · Fishery stock · Global warming · Numerical simulation · Japan Sea

1 Introduction

Climate changes have significant effects on marine ecosystems and fishery resources (Blanchard et al. 2012; Barange et al. 2014; Cheung 2018; Moore et al. 2018). As a sub-

---

Electronic supplementary material The online version of this article (https://doi.org/10.1007/s10584-020-02689-3) contains supplementary material, which is available to authorized users.

✉ Xinyu Guo
guoxinyu@sci.ehime-u.ac.jp

Extended author information available on the last page of the article polar region, the Japan Sea (JS) exhibits more pronounced warming than other regions (Japan Meteorological Agency 2018). The mean value of the sea surface temperature (SST) in the JS increased at a rate of 1.08 °C/century from 1891 to 2012, which is twice that of the corresponding value in the other waters (Wakamatsu et al. 2017). With such significant environmental changes, the fishery resources in Japan has been reported to have decreased by ~35% from 1930 to 2010, making it one of the largest declines in the world (Free et al. 2019).

The Japanese flying squid (*Todarodes pacificus*) is an important fishery species in East Asia. Its catch records are available from the early 1900s in Japan and beginning in the 1930s in Korea. According to these records, the annual catch exhibited several different phases in the past 100 years: at a low-abundance phase (less than 200 thousand tons) before the 1940s, increasing to a high-abundance phase (approximately 400 thousand tons) from the early 1950s to the end of the 1960s, and decreased gradually from the highest catch of 668 thousand tons in 1968 to the lowest catch of 90 thousand tons in 1986 (Murata 1989). After 1986, the catch of Japanese flying squid increased again and returned to a high level of ~400 thousand tons in the 1990s and the early 2000s (Kidokoro et al. 2010). Recently, the catch from 2010 to 2018 has shown a new decreasing trend (Fisheries Agency of Japan and Japan Fisheries Research and Education Agency 2018) and this has widely raised social concerns regarding its future production.

A climate regime shift was suggested to be the main cause for the variation in the amount of stock (Sakurai et al. 2000; Kidokoro 2003; Kidokoro et al. 2010; Rosa et al. 2011). Sakurai et al. (2000) suggested that the change in fishery resources of the Japanese flying squid was controlled by the spawning area. Their study showed that the density of paralarvae in the northern part of the East China Sea (ECS) and the southwestern part of the JS in autumn had a significant positive relationship ($R^2 = 0.91$, $p < 0.01$) with annual catches of the autumn-spawning cohort in the JS. The increasing catch of Japanese flying squid since the late 1980s is consistent with expansion of spawning grounds for the autumn- and winter-spawning cohorts. The direct reason for the expansion of spawning grounds is the increasing regional water temperature along with a climate regime shift (Sakurai et al. 2000). In addition to water temperature, the prey conditions are also important to the growth of Japanese flying squid. Kang et al. (2002) reported a good correlation between annual catch of squid and zooplankton biomass in the previous year.

Using the survival and growth conditions for Japanese flying squid provided by cultivation experiments (Watanabe et al. 1996; Sakurai et al. 1998), it is possible to develop a numerical model to consider the effects of water temperature and prey conditions on Japanese flying squid. Kishi et al. (2009) proposed a bioenergetics model for Japanese flying squid and coupled it with a low trophic ecosystem model to assess the change in the production of Japanese flying squid in relation to global warming. Their model focused on the response of physiological processes of squid to global warming; therefore, it fixed the spawning grounds and migration route of the squid, both of which likely change with global warming because of their high dependence on water temperature and the flow field. In addition, their model does not include ontogenetic vertical migration (OVM) and temperature-dependent survival rate. Kim et al. (2015) used a particle tracking model to simulate the migration route and spatial distribution of larvae of Japanese flying squid. Their model included OVM and temperature-dependent survival rates but did not consider the physiological processes of squid larvae.

For the JS, the increase rate in annual mean SSTs is ~1.71 °C per century in the central part and ~1.29 °C per century in the southwestern part in the past 100 years (Climate Change

Monitoring Report 2017 by the Japan Meteorological Agency, https://www.data.jma.go.jp/gmd/kaiyou/english/long_term_sst_japan/sea_surface_temperature_around_japan.html). Moss et al. (2010) proposed four Representative Concentration Pathways (RCPs) for possible socio-economic development states in the future. RCP2.6 assumes a low level of CO_2 emissions that increases the global annual mean surface temperature by 0.3–1.7 °C by the end of the twenty-first century compared with that at the end of the twentieth century. RCP8.5 assumes a high level of CO_2 emissions that increase the global annual mean surface temperature by 2.6–4.8 °C. RCP4.5 and RCP6 are between the above two extreme scenarios (Van Vuuren et al. 2011). Because the current emission rate was reported to be close to that of RCP8.5 (Peters et al. 2012), we have to meet a situation with a stronger warming intensity than before. According to the results of climate model intercomparison project (CMIP) 5 under the RCP8.5, the annual mean SST in the JS will increase by at least 3.5 °C by the end of the twenty-first century compared with that at the end of the twentieth century (Mizuta et al. 2014).

Against background of reduction in Japanese flying squid catch in recent years and dramatic changes in the seas around Japan over the next 100 years, we used an individual-based model (IBM) to examine the change in spawning grounds and resource of the squid in the twenty-first century. In our simulation, we coupled the IBM, which contains the physiological processes of Japanese flying squid, with a behavioral-hydrodynamic model that includes the transport and survival processes of the larvae of Japanese flying squid.

The model structure and the data used are described in Section 2; Section 3 presents the calculated results; Section 4 discusses the causes for the changes in squid resources in the future.

2 Model and data

2.1 IBM

In this study, we used a particle to represent a squid larva and released particles in the place whose water depth and sea surface temperature meet the condition for spawning of squid (Supplementary Material 1). The movement of particles is controlled by ocean current, random walk, and OVM (Supplementary Material 1). In addition to migration, we also applied an ontogenetic model to each particle to incorporate the temperature-dependent survival process and the physiological processes affecting the wet weight of squid (Supplementary Material 1). The model simulated the early life stage of squid for 182 days. Kidokoro et al. (2014) indicated that there was a positive correlation between the number of young squid and the number of harvestable squid.

The calculation for a year started on January 1, followed by another 36 times when particles were released for 10-day intervals. Particles released from January to March were defined as the winter-spawning cohort, from April to June as the spring-spawning cohort, from July to September as the summer-spawning cohort, and from October to December as the autumn-spawning cohort.

2.2 Field data for IBM

To simulate the migration of the Japanese flying squid larvae, we needed water temperature and ocean current velocity for each case. We also needed the density of zooplankton and water temperature as input data for the ontogenetic model for squid. For such purpose, we used the RIAM ocean model (RIAMOM) (Lee et al. 2003, Hirose et al. 2013, https://dreams-c.riam.kyushu-u.ac.jp/vwp/) to obtain time-varying, 3-dimensional fields of ocean current velocity, water temperature, and zooplankton density whose daily means were saved in one-day interval for the use of IBM model. The 3-dimensional field data has a resolution of 1/12° in the zonal direction, 1/15° in the meridian direction, and 38 layers in the vertical direction and covers the ECS, the JS, and part of the Kuroshio area south of Japan (Fig. 1).

The RIAMOM was initially designed to simulate the physical variables in the JS (Lee et al. 2003). Recently, it has included a low-trophic ecosystem module for the study on dissolved oxygen in the JS (Kim et al. 2019). Using RIAMOM and its ecosystem module, we designed six cases for the calculation corresponding to different climate conditions. Case 1960s was for the period of 1960–1966, whereas case 2010s was for the period of 2008–2013. Case 1960s was an example of a high-abundance phase while case 2010s was a low-abundance phase.

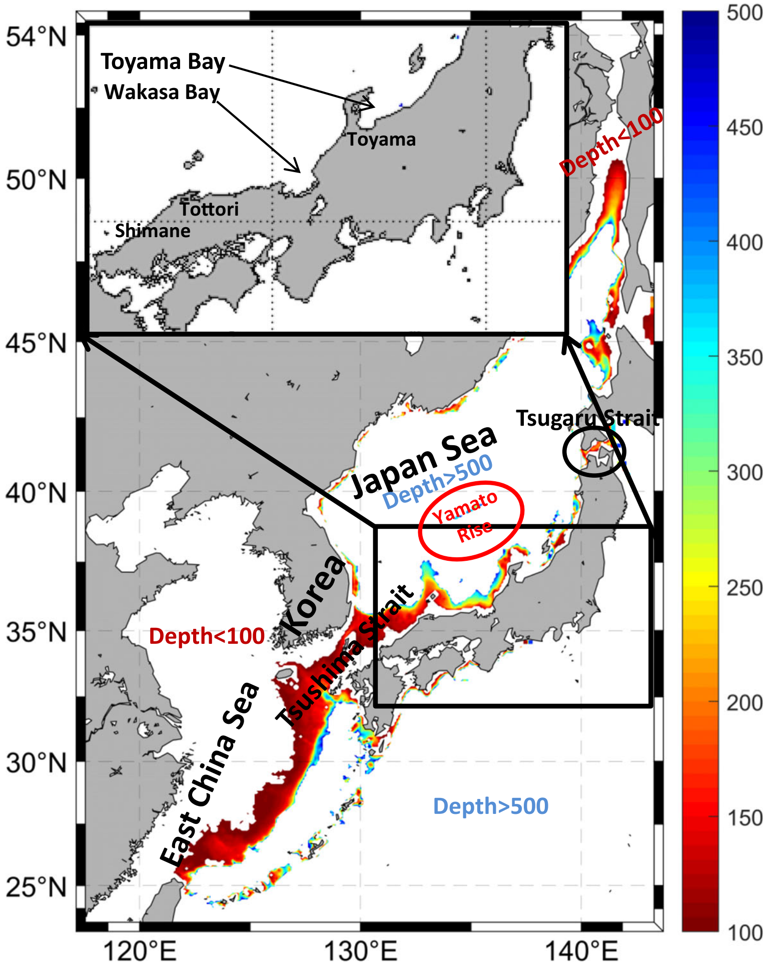

Fig. 1 The topography of the area under study. The colored area is within a water depth of 100–500 m, which is a potential area for spawning grounds. If the SST in this area is in the range of 19.5–23 °C, it will become a spawning ground for the squid

These two cases were designed for comparisons with 4 warming cases. In addition, case 2010s was also used to compare with the resource data of squid to verify our IBM model. Case 2050s-2.6 and case 2100s-2.6 were based on the RCP 2.6 warming prediction for the period of 2056–2061 and 2104–2109, respectively; case 2050s-8.5 and case 2100s-8.5 were for the RCP8.5 warming prediction for the period of 2056–2061 and 2104–2109, respectively.

The air-sea boundary conditions in cases 1960s and 2010s were calculated from JRA55 (Kobayashi et al. 2015) that provides winds, air temperature, specific humidity, precipitation, long-wave radiation, and short-wave radiation from 1956 to 2015 with an interval of 3 h. In the warming cases, except for the air temperature and specific humidity, the other air-sea boundary conditions were kept the same as those in case 2010s. In two cases of RCP2.6, the air temperature and specific humidity were increased by 1 °C and 1.5%, respectively; in two cases of RCP8.5, they were increased by 2 °C and 3% in case 2050s-8.5, and by 4 °C and 6% in case 2050s-8.5, respectively. The lateral boundary conditions and initial conditions for the above 6 cases were from an ocean model with a coarse grid but a larger domain (northwestern Pacific Ocean), which has been run continuously from 1958 to 2111 with a similar configuration for air-sea boundary conditions (Kim et al. 2019).

3 Results

In this study, we defined the particle surviving to day 182 (i.e., end of each calculation) as young squid and their total number in the JS was the young stock or number of young squid. The model has been validated to be able to reproduce the interannual variations in the number of young squid in the JS (Supplementary Material 2).

3.1 Spawning of Japanese flying squid

The first effect of ocean warming on the squid in our model is the release of particles at day 0. It represented the amount of spawning and spawning grounds, which have been used as indexes for examining the change in the common squid resource with SST (e.g., Rosa et al. 2011). The amount of spawning showed a slightly decreasing trend with warming (first column in Table 1). For example, it decreased by 2.8% in case 2100 s-2.6 and by 5.3% in case 2100 s-8.5 as compared with that of case 2010s.

Table 1 Summary of spawning, migration, survival, and mortality. The budget for Japanese flying squid in the JS by percentage

Cases	Spawning (particle abundance)	Migration into JS (particle abundance)	Number of young squid (particle abundance)	Low-temperature mortality (%)	High-temperature mortality (%)	Flow out	Survival to young squid stage (%)
1960s	3.31×10^5	1.43×10^5	5.13×10^4	46.9	14.5	2.6	36.0
2010s	3.21×10^5	1.33×10^5	4.34×10^4	49.1	16.6	1.7	32.6
2050s-2.6	3.12×10^5	1.36×10^5	5.70×10^4	36.9	17.5	3.6	42.0
2100s-2.6	3.12×10^5	1.40×10^5	6.01×10^4	34.1	19.5	3.4	43.0
2050s-8.5	3.12×10^5	1.36×10^5	6.49×10^4	32.2	17.0	3.2	47.6
2100s-8.5	3.04×10^5	1.39×10^5	7.79×10^4	18.8	22.0	3.3	55.9

Because the autumn-spawning cohort is the main contributor to the annual stock size, we show the change of its spawning area with warming (Fig. 2). In case 2010s, spawning occurred along the shelf area in the ECS and the JS, ranging from north of Taiwan to the south coast of the JS offshore of Toyama (Fig.2b). In case 1960s, the spawning density in the ECS was higher than that in case 2010s, whereas that in the JS was lower than that in case 2010s (Fig.2a). For the warming cases, a decrease in spawning density occurred throughout the spawning grounds. The reduction of spawning density was larger in case 2100 s than in case 2050s for both RCP 8.5 and RCP 2.6, whereas it was larger in both cases for RCP 8.5 than in those for RCP 2.6. Spatially, the reduction is greater in the southern area than in the northern area. The largest reduction occurred in the spawning grounds north of Taiwan. We also show the changing of spawning areas in other seasons with warming in S-Figs.2-4 in Supplementary Material 3 whose caption gives necessary description on these results.

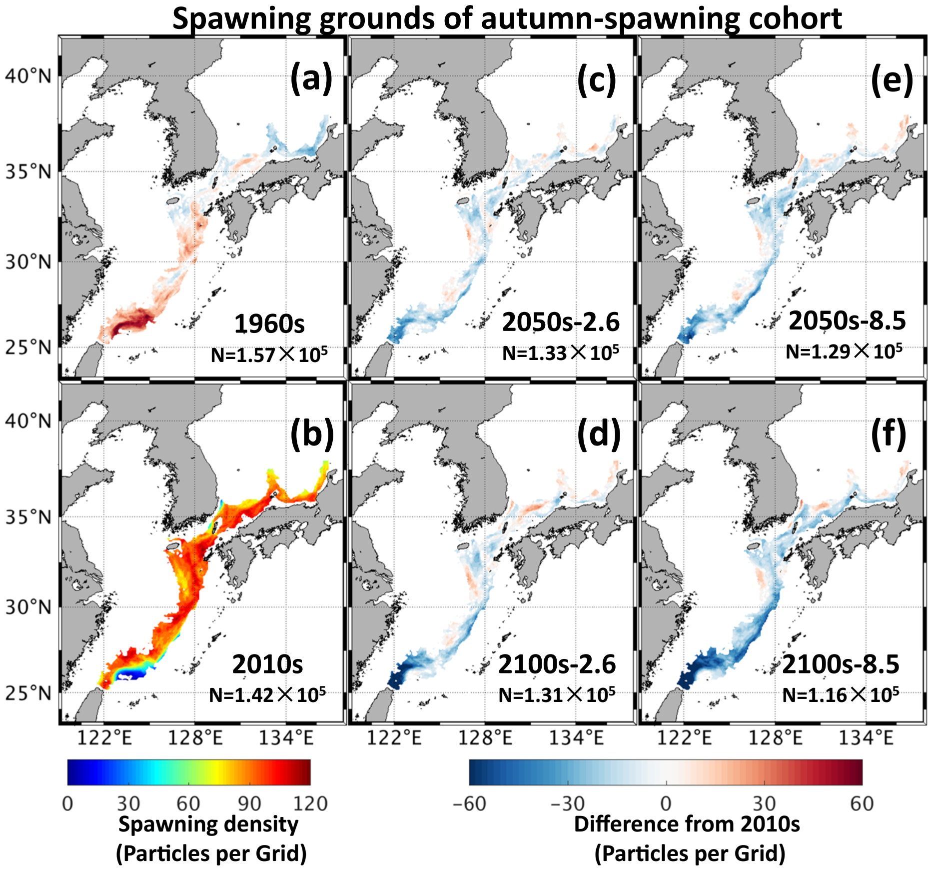

Fig. 2 Autumn-spawning larvae particles in the six cases. Color in **(b)** denotes the spawning density (number of particles per grid point) in Case 2010s averaged from 2008 to 2014. **a**, **c**, **d**, **e**, and **f** are cases 1960s (average of 1960–1966), 2050s-2.6 (average of 2056–2062), 2100 s-2.6 (average of 2104–2110), 2050s-8.5 (average of 2056–2062) and 2100 s-8.5 (average of 2104–2110). Color in (**a**), (**c**), (**d**), (**e**), and (**f**) denotes the difference between the respective case and that of Case 2010s. N is the sum of the spawned particles over the entire spawning ground

The temporal variation in the amount of spawning also changed with warming (Fig. 3). The amount of spawning had two peaks. The first peak denoted larvae spawned from late May to June and became young squid in late November to December. The second peak denoted larvae spawned in mid-November and became young squid in May of the following year. We called the first the spring peak and the second the autumn peak in this study.

The spring peak tended to occur earlier with warming. In cases 1960s and 2010s, it was in late June; in cases 2050s-2.6, 2050s-8.5, and 2100s-2.6, it occurred 10 days earlier and in case 2100s-8.5, it occurred 20 days earlier than that of case 2010s. On the other hand, the autumn peak tended to be delayed with warming. In case 1960s, the autumn peak occurred in late October, remaining at a high value from mid-October to early November. Compared with that of case 1960s, it was delayed by 10 days in cases 2010s, 2050s-2.6, and 2050s-8.5 and by 20 days in cases 2100s-2.6 and 2100s-8.5. In case 2100 s-2.6, the amount of spawning reached a high level 10 days before the peak. In the case 2100 s-8.5, the amount of spawning maintained a high value for 10 days after the autumn peak.

The amount of spawning in each season is presented in S-Table 1 in Supplementary Material 3 as a quantitative summary of Fig. 3. Firstly, there was apparent seasonal variation. For example, in case 2010s, the amount of spawning in spring and autumn represented the majority of the annual amount of spawning, accounting for 34% and 44% of the annual spawning. The winter-spawning cohort accounted for 18%, whereas the amount of spawning in summer accounted for 4%.

The amount of spawning for the winter-spawning cohort increased significantly in warming cases. Compared with that of case 2010s, the winter-spawning cohort increased the amount of spawning by 11% in case 2050s-2.6, by 28% in case 2100s-2.6, by 22% in case 2050s-8.5, and by 49% in case 2100s-8.5. In contrast, the amount of spawning in other seasons showed a

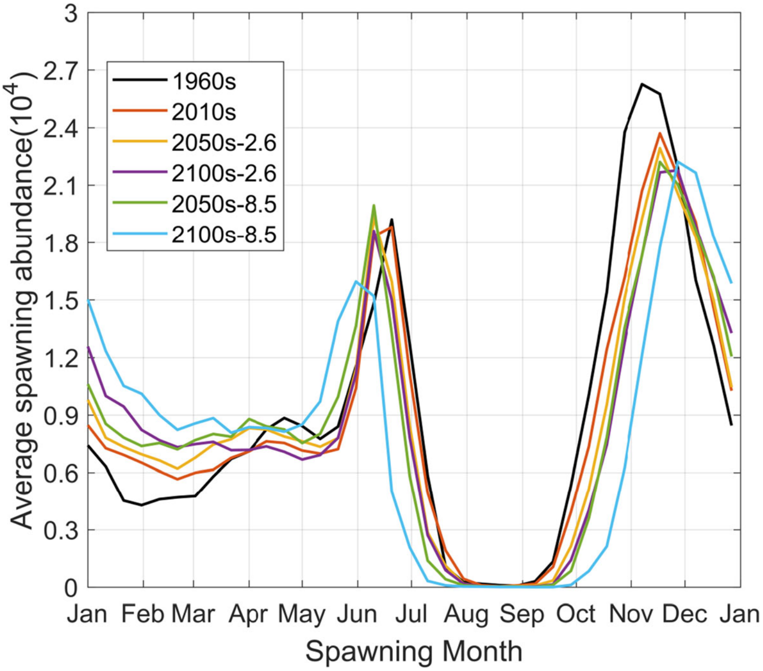

Fig. 3 Average spawning abundance (numbers of particles released) by case, lagged to the spawning date

reduction with warming. For example, compared with that of case 2010s, the autumn-spawning cohort reduced the amount of spawning by 6% in case 2050s-2.6, by 7% in case 2100 s-2.6, by 9% in case 2050s-8.5, and by 18% in case 2100s-8.5.

3.2 Young squid stock in the JS

The number of young squid in the JS varied with spawning seasons (Table 2**).** The autumn-spawning cohort had the largest stock size, accounting for ~70% of the annual number of young squid in the JS in all six simulations. The spring-spawning cohort was in the second position, accounting for 20% of the annual number of young squid in case 2010s, which decreased with warming to 15% in case 2100 s-8.5. The winter-spawning cohort was in the third position, accounting for ~7% of the annual number of young squid in case 2010s, which increased with warming to 14% in case 2100s-8.5. The summer-spawning cohort made the smallest contribution, accounting for only ~2% of the annual number of young squid in case 2010s, which declined to zero in case 2100s-8.5.

The distribution area of young squid showed a northward extension with warming (Fig. 4 and S-Figs. 5-7 in Supplementary Material 3). Being the largest contributor to the annual stock size, the autumn-spawning cohort was distributed over the entire area south of the polar front in the JS, west of the Korean coast, and east of the Japanese coast (Fig. 4). The highest density of young squid was located in the offshore area of Japan, moving northeastward along the Japanese coast with warming. In cases 1960s (Fig.4a) and 2010s (Fig.4b), the highest density was located in the offshore area of Shimane and Tottori. In cases 2050s-2.6 (Fig.4c) and 2050s-8.5 (Fig.4e), the highest density was located in the offshore area near Wakasa Bay and the southern part of Yamato Rise (latitude, 37.5–40.3° N; longitude, 133.3–135.0° E). In cases 2100s-2.6 (Fig.4d) and 2100s-8.5 (Fig.4f), the highest density was located in the offshore area near Toyama Bay.

Not only the highest density area but also the northern boundary of the young squid moved northward with warming. For example, besides those near the Tsugaru Strait, the young squid were distributed south of 40° N in cases 1960s and 2010s. In cases 2050-2.6 and 2050-8.5, the young squid were distributed near the offshore area of the Korean Peninsula around 40° N. In cases 2100s-2.6 and 2100s-8.5, the young squid were distributed north of 40° N. Except for the summer-spawning cohort, who could not survive under future warming conditions, the

Table 2 Young stock of each seasonal spawning cohort and its annual percentage in all cases

Young stock (annual Percentage)	**Cases**					
	1960s	2010s	2050s-2.6	2100s-2.6	2050s-8.5	2100s-8.5
Total abundance	5.13×10^4	4.34×10^4	5.70×10^4	6.01×10^4	6.49×10^4	7.79×10^4
Winter	3.20×10^3	3.35×10^3	5.10×10^3	6.99×10^3	6.20×10^3	1.12×10^4
	(6.2%)	(7.7%)	(9.0%)	(11.6%)	(9.6%)	(14.3%)
Spring	1.23×10^4	9.52×10^3	1.13×10^4	1.10×10^4	1.34×10^4	1.19×10^4
	(23.9%)	(21.9%)	(19.8%)	(18.4%)	(20.7%)	(15.3%)
Summer	1.01×10^3	1.03×10^3	6.10×10^2	3.73×10^2	2.41×10^2	2.63×10^1
	(2.0%)	(2.4%)	(1.1%)	(0.6%)	(0.4%)	(0.0%)
Autumn	3.48×10^4	2.95×10^4	3.99×10^4	4.17×10^4	4.50×10^4	5.48×10^4
	(67.8%)	(68.0%)	(70.1%)	(69.4%)	(69.4%)	(70.4%)

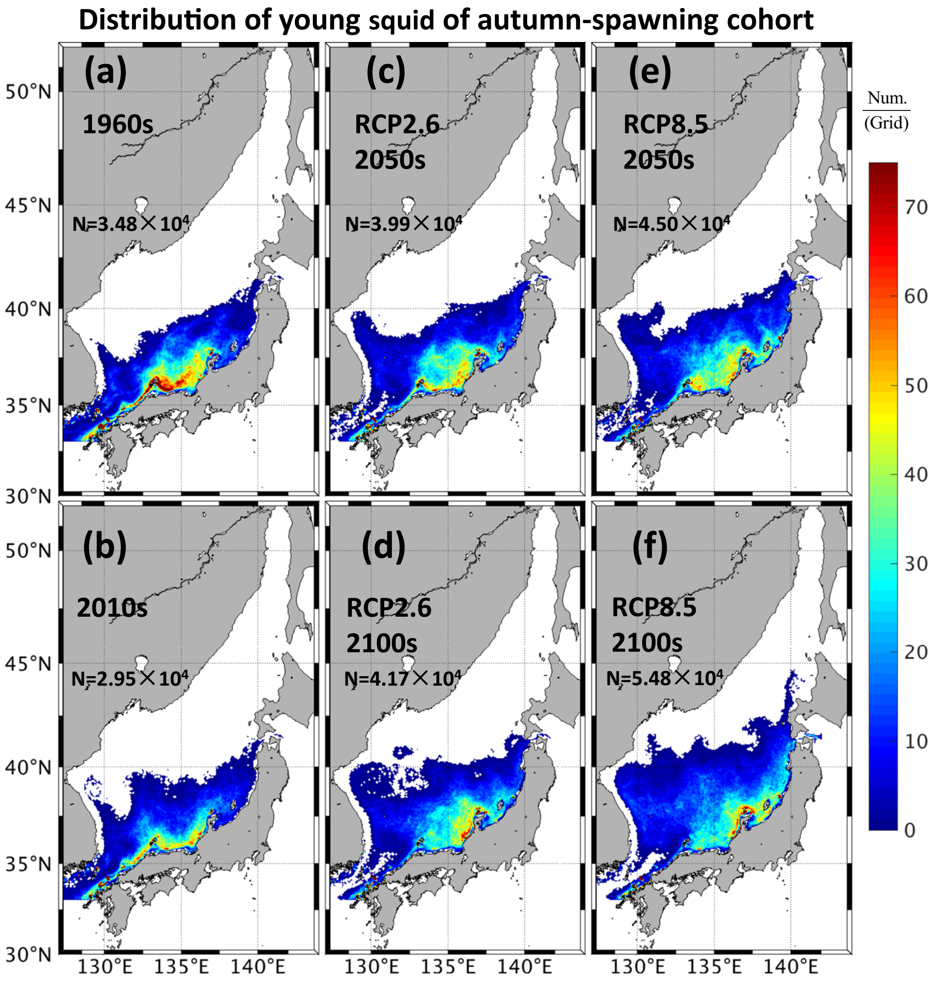

Fig. 4 Distribution of young squid of the autumn-spawning cohort. **a**, **b**, **c**, **d**, **e**, and **f** correspond to cases 1960s, 2010s, 2050s-2.6, 2100s-2.6, 2050s-8.5, and 2100s-8.5. Color denotes the averaged density of young squid over the years in each case, which is the number of live particles per grid point after 182 days of simulation. *N* is the sum of the number of particle

cohorts spawned in other seasons (S-Figs. 5-7 in Supplementary Material 3) showing a similar northward movement as the autumn-spawning cohort (Fig. 4).

To obtain a continuous image regarding how the young squid depended on the spawning time, we present their total number (= young squid amount) in the JS versus their spawning time that is 182 days ahead of the time for calculating young squid amount (Fig. 5). Like the spawning peaks in Fig.3, there were also spring and autumn peaks in the number of young squid amount over a year. For the spring peak, the maximum value of the young squid amount had no apparent variation among the six simulation cases. For the autumn peak, however, the maximum value of young squid amount increased significantly with warming: ~ 6000 in case 2010s, ~ 7000 in case 1960s, ~ 8000 in cases 2050s-2.6 and 2100s-2.6, ~ 9000 in case 2050s-8.5, and ~ 12,000 in case 2100s-8.5. The winter-spawning cohort, especially the squid spawned in January, apparently increased with warming. In contrast, the summer-spawning cohort could not survive in warming cases.

Table 2 summarizes the results shown in Fig. 5 according to the spawning season. The winter-spawning cohort had an apparent increase with warming. Compared with case 2010s (low-abundance phase), its stock size was 52% higher in case 2050s-2.6, 85% higher in case 2050s-8.5, 108% higher in case 2100s-2.6, and 233% higher in case 2100s-8.5. Compared with case 1960s (high-abundance phase), these values became 59%, 94%, 118%, and 248%, respectively.

The spring-spawning cohort had no clear increasing trend with warming as did the winter-spawning cohort. Compared with case 2010s, future cases showed an increase in the number of young squid: 19% in case 2050–2.6, 41% in case 2050–8.5, 16% in case 2100–2.6, and 25% in case 2100–8.5. However, compared with case 1960s, the three future cases showed a decrease in the number of young squid: − 8% in case 2050s-2.6, − 10% in case 2100 s-2.6, and − 3% in case 2100 s-8.5. An increase occurred only in case 2050-8.5 (9%). The summer-spawning cohort showed a simple response to warming, by going extinct in the future (Table 2).

The autumn-spawning cohort showed an increase with warming. Compared with case 2010s, its stock size increased by 35% and 41% in 2050s and 2100 s, respectively, under RCP 2.6 and by 53% and 86% in 2050s and 2100 s, respectively, under RCP 8.5. Compared with case 1960s, the increase was 15% in case 2050s-2.6, 20% in case 2100-2.6, 29% in case 2050-8.5, and 57% in case 2100-8.5.

Table 2 also shows a comparison for the change in stock size from the high-abundance phase (1960s), low-abundance phase (2010s), and those from the 2010s to 2050s and from the

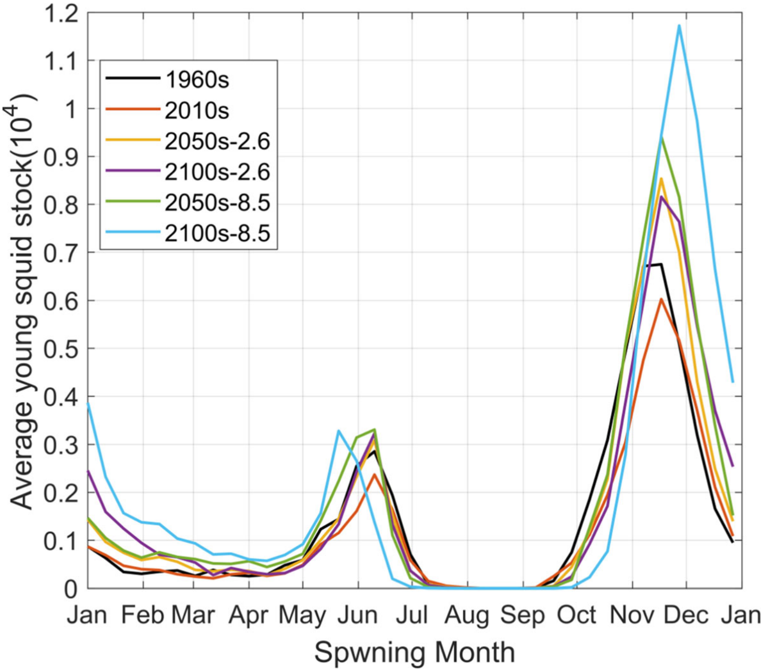

Fig. 5 Average young squid stock (= number of particles surviving for 182 days) in the Japan Sea by case, lagged to spawning date

2050s to 2100s. The winter- and autumn-spawning cohorts exhibited a consistently increasing trend with warming. Their increasing range from the 2010s to 2050s and from the 2050s to 2100s under RCP 2.6 and RCP 8.5 were generally larger than the difference between the high-abundance phase (1960s) and low-abundance phase (2010s), indicating a larger warming effect than that previously experienced.

4 Discussions

4.1 The mechanism for the increase in the number of young squid

Our simulations showed that although the number of spawned larvae decreased slightly with warming in the future, the number of young squid in the JS increased significantly (Table 1). Here, we present the causes for the increase in the number of young squid in our model.

The number of young squid in the JS depended on the particles spawning in and entering the JS as well as their survival rate up to the end of each simulation. Figure 6a displays the variation in the total number of particles, including both alive and dead larvae, inside the JS at the end of each simulation, which represents the particles spawning in and entering the JS. If we compare the total numbers of particles in the JS (Fig. 6a) with those of spawned particles (Fig. 3), their ratio is ~2/3 for the spring- and autumn-spawning cohorts. Consequently, the autumn peak in Fig. 6a is only slightly higher than that of the spring peak, which cannot explain the apparent difference in the spring and autumn peaks of young squid amount in Fig. 5. Further, either the spring-spawning cohort or the autumn-spawning cohort did not show a clear change in the total number of particles in the JS with warming (Fig. 6a). Therefore, the change in the particles spawning in and entering the JS is not the cause of the increase in the number of young squid with warming (Fig. 3 and Table 2).

The significant change in the number of young squid among the six cases was caused by the increased survival rate of larvae in the JS. Figure 6b shows the amount of mortality for squid larvae inside the JS in all cases, among which the autumn-spawning cohort presented an

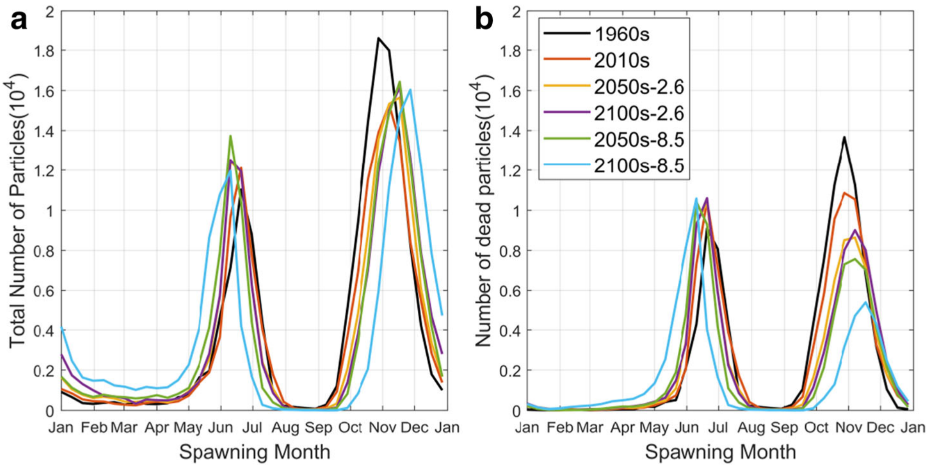

Fig. 6 Number of larvae particles inside the Japan Sea at the end of each simulation. **a** Both alive and dead particles. **b** Number of dead particles. Abscissa is spawning time

apparent change with warming: its peak value decreased and its peak time was delayed. The spring-spawning cohort advanced its peak time but exhibited little change in total mortality number (Fig. 6b). In the projected future warming cases, the autumn-spawning cohort had significantly lower mortality than did the spring-spawning cohort, which is the cause why the autumn-spawning cohort had a higher peak value for the number of young squid than did the spring-spawning cohort in warming cases (Fig. 5).

There are three factors that prevented a particle from becoming a young squid inside the JS. As introduced in Supplementary Material 1, the particle was judged to be dead if the water temperature surrounding the particle was higher than the high limit or lower than the low limit. We named them as mortality due to high temperature (MHT) and mortality due to low temperature (MLT). In addition to these two factors, the particle can be also transported out of the JS (flow out).

For the particles transported into or spawned inside the JS in the 1960s and 2010s, the winter-spawning cohort had the lowest loss rate (~ 5–18%), followed by the autumn-spawning cohort (~ 60%), spring-spawning cohort (~ 70–80%), and summer-spawning cohort (> 90%). MHT was the major factor for the loss of the spring- and summer-spawning cohorts, while MLT was the major factor for the loss of the autumn-spawning cohort (S-Fig. 8 in Supplementary Material 3).

With warming, the proportion of MHT increased but that of MLT decreased (Table 2). This change was greater in both cases for the 2100s than those for the 2050s and greater in cases for RCP8.5 than those for RCP2.6. As a major reason for the loss of the autumn-spawning cohort, MLT rapidly decreased with warming, which made the survival rate of the autumn-spawning cohort increase rapidly. This increase alone was able to explain the majority of the increase in the annual number of young squid. For example, the MLT for the autumn-spawning cohort decreased from 62% in case 2010s to 31% in case 2100s-8.5. This process increased the number of young squid in the autumn-spawning cohort by 3.12×10^4 for case 2100s-8.5, which explains 90.4% of the increase relative to that of case 2010s (S-Fig. 8 in Supplementary Material 3).

Pörtner and Knust (2007) mentioned that cold water species at high latitudes usually benefit from warming. Our simulations suggest that Japanese flying squid in the JS follows this rule. At least for the next 100 years, the water temperature conditions under the warming scenarios favor the increase in the number of young squid in the JS.

4.2 Change in temperature experienced by squid larvae under warming conditions

To understand the benefit of warming, it is necessary to examine the temperature experienced by the squid larvae along their migration route. Variation in the temperature over the next 100 years is also a prerequisite for understanding the response of the squid's physiological processes to warming, which will be addressed in Section 4.3.

Using the recorded water temperature at the position of each particle during its calculated duration of 182 days, we obtained the mean temperature experienced by all the particles that were alive at the end of each simulation. We then averaged them according to season in the six cases based on days passed since release and presented the mean temperature experienced for an interval of 20 days (Fig. 7). Using case 2010s as an example, the summer-spawning cohort showed a continuous reduction in its mean experienced temperature, whereas the other seasonal cohorts experienced a reduction at the beginning of the calculation but then an increase in their mean experienced temperature. Specifically, the winter-spawning cohort had an average release time in February. Its mean experienced temperature began with a value of ~ 19 °C, dropped to a low value of ~ 16 °C after 80–100 days (May), and then increased to a value of ~ 18 °C by the end of the calculations (August). The experienced temperature for the spring-spawning cohort began at ~ 20 °C, dropped to ~ 16 °C after 80–100 days (August), and subsequently increased to ~ 17 °C. That of the summer-spawning cohort began at ~ 21 °C and dropped linearly to ~ 12 °C after 160–180 days (February). The mean release date of the autumn-spawning cohort was in November. Its mean experienced temperature began at ~ 20 °C, dropped to ~ 12 °C after 120–140 days (March), and increased to ~ 13 °C after 160–180 days (June).

Three factors were able to explain the variation in mean experienced temperature of larvae particles. Larvae particles moved northward in all cohorts, and their experienced water temperature generally decreased with increasing latitude. Seasonal variation in water temperature also affected the temperature experienced by larvae particles. OVM caused larvae particles to remain at different depths as a response to changes in their life stages. With the change of depths, the experienced temperature also varied. In the early stage of the simulation, migration is fast because of the strong current. At the late stage of the simulation, the migration speed of particles was relatively slow (Fig. 8 and S-Fig. 9 in Supplementary Material 3).

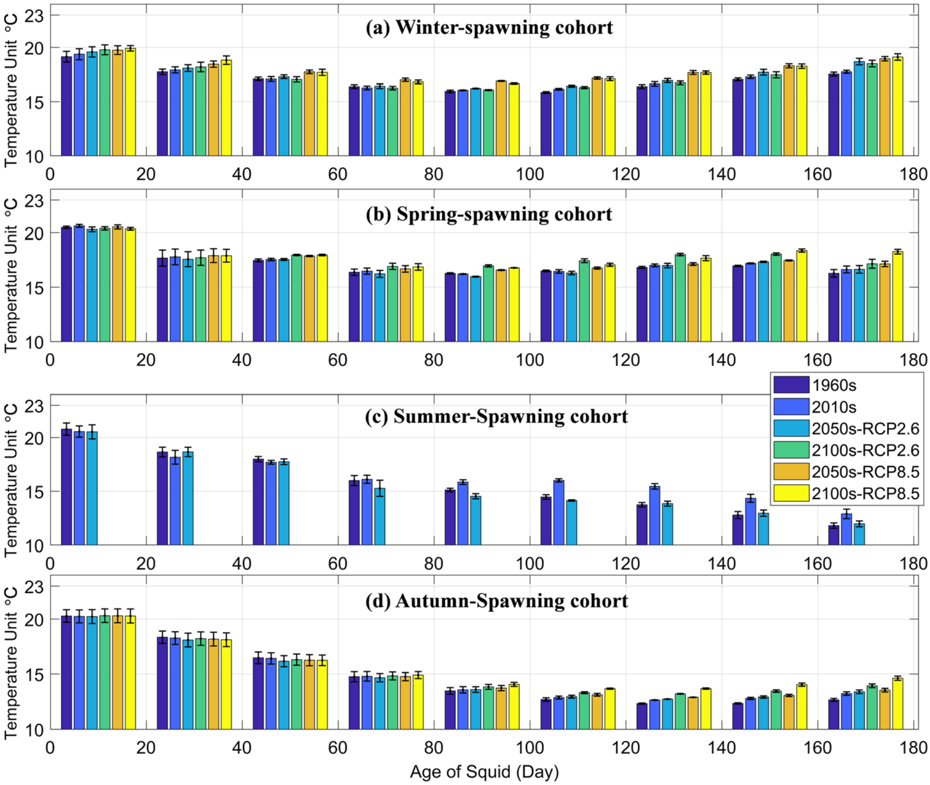

Fig. 7 Time series of average water temperature experienced by individuals. **a**, **b**, **c,** and **d** correspond to the spawning season of winter, spring, summer, and autumn. The colors from dark blue to light yellow represent cases from 1960s to 2100s-8.5. Color bar represents the mean of water temperature experienced within 20 days, whereas the error bar above it represents the standard deviation of the water temperature

Therefore, the experienced temperature of larvae particles was mainly influenced by the latitudinal factor in the early stage of simulation, and by the seasonal factor in the later stage. OVM led to two jumps in the depth of larvae particles on the 20th and 60th days of the simulation, and the increased depth at the two jumps led to a reduction in the experienced temperature, which was more apparent in spring and summer than in autumn and winter because of the presence of a strong stratification.

In our simulations of warming cases, the increase in the temperature experienced by larvae particles was less than the increase of mean water temperature in the JS due to warming. Using the autumn-spawning cohort as an example again, the experienced temperature of larvae particles was not affected by warming during 0–80 days (Fig. 7d). This was because the northward movement of the migration route with warming was generally synchronized with the warming-induced northward movement of isotherms (Fig. 8). During 80–180 days, the experienced temperature of larvae particles increased with warming, and the range increased

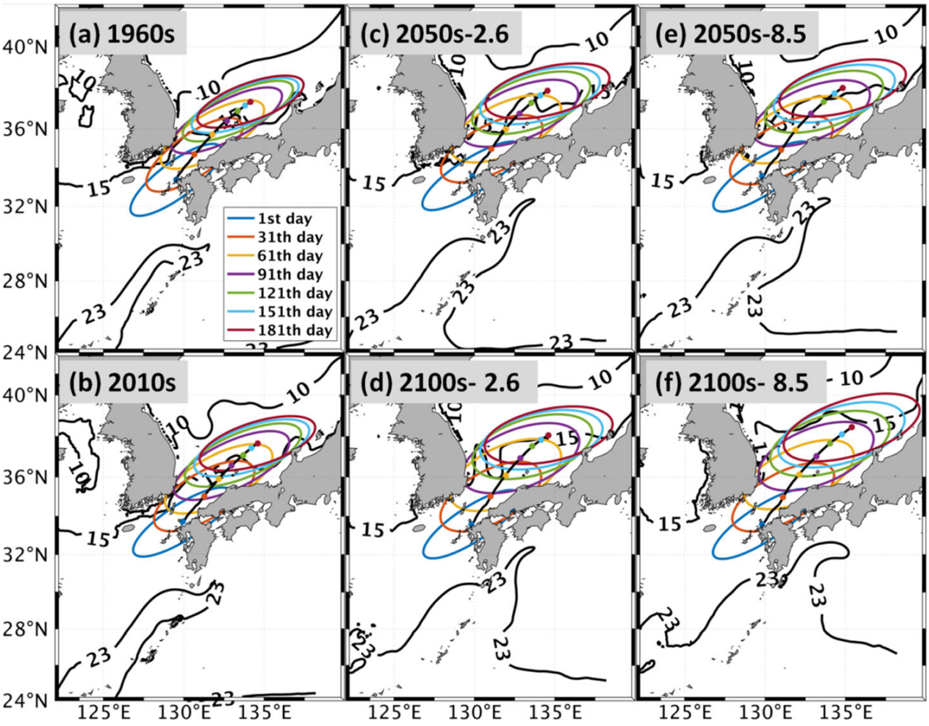

Fig. 8 The migration route of the autumn-spawning cohort in the six cases. The daily horizontal positions for all particles that were released in autumn (October–December) and eventually were alive in the Japan Sea were averaged to obtain the mean migration route over the 182 days of simulation. The 182 averaged locations are represented by the black line inside the ellipses, which represent the standard deviation of the distribution of particles. The radius of the major axis of the ellipse represents the standard deviation in the direction of maximum dispersion. The direction of the major axis of an ellipse is the same as that of the maximum variance. The radius of minor axis of the ellipse represents the standard deviation in the direction of minimum dispersion. The ellipses were plotted every 30 days along the trajectory. Colors of ellipses are used to distinguish different dates. The average position of the particles on a day, i.e., center of the ellipse, is represented by points in the same color. The black lines with number indicate the annual mean temperature for the layer (0–100 m) where the squid larvae particles existed. The reason we plotted isotherm of 10 °C, 15 °C and 23 °C is because the maximal spawning and surviving temperate is 23 °C and the minimum surviving temperature is between 10 and 15 °C in different life stage. In addition, 10–15 °C is the OGTR for the early life stage of Japanese flying squid

with the number of tracked days. However, compared with case 2010s, the maximum increase of experienced temperature was less than 2 °C in case 2100s-8.5, which was lower than that of the 4 °C reported by Kishi et al. (2009).

The main reason for the difference in temperature experienced by squid larvae between our study and that of Kishi et al. (2009) was because the IBM simulation in this study presented a northward shift of the migration route of the squid larvae with warming (Fig. 8 and S-Fig.9 in Supplementary Material 3), which was however not considered by Kishi et al. (2009) who used a fixed migration route for the squid larvae.

There are two processes responsible for the northward shift of the migration route. First, the flow and water temperature fields in the JS changed with warming (Kim et al. 2019; Mao et al. 2019), and the enhanced Tsushima Current in the warming cases (S-Fig. 10 in Supplementary Material 3) brought the particles further to the north than in cases 2010s and 1960s. Second, the northward shift of the spawning grounds made it easy for particles to follow the northward currents into the JS. For example, more particles from the winter-spawning cohort entered the JS rather than went to the Kuroshio area in the warming cases.

4.3 Effects of warming on physiological processes and individual weight

Kishi et al. (2009) examined the influences of warming on the physiological processes of the autumn-spawning cohort. Because warming will increase the energy loss of squid through respiration, Kishi et al. (2009) suggested that squid wet weight would decrease with warming. However, our simulations predicted that the weight of young squid would not decrease in the next 100 years, although we used the model by Kishi et al. (2009) as an individual growth module in our simulation system. The different temperatures experienced by squid particles caused a different effect on the physiological processes and individual weight of the squid.

Table 3 summarizes the mean individual weight and mean life-long metabolic amount of physiological processes of the alive larvae particles in the six cases. The weight of squid is low in case 1960s but high in case 2010s. The weight in four warming cases was slightly lower than that of case 2010s but was higher than that of case 1960s. In fact, the weight of young squid of the autumn-spawning cohort increased slightly with warming (S-Fig. 11a in Supplementary Material 3**)**. For example, in the four warming cases, the individual weight was higher in the two 2100 s cases than in the 2050s cases, in both cases for RCP 2.6, and those for RCP 8.5. Because the number of young squid in the autumn-spawning cohort accounted for ~ 70% of that of the entire year, the change in individual weight in the autumn cohort was the leading factor in the annual mean individual weight.

Table 3 Mean and standard deviation of life-long physiological processes and individual wet weight, all of them was averaged across all larvae particles in each case. The percentage represents the proportion of the physiological process to the total consumption in mean value

Cases	Wet weight (g/squid)	Consumption (g/squid)	Respiration (g/squid)	SDA (g/squid)	Egestion (g/squid)	Excretion (g/squid)
1960s	50 ± 18 (57%)	88 ± 33 (100%)	12 ± 6 (14%)	14 ± 5 (16%)	4 ± (5%)	7 ± 3 (8%)
2010s	61 ± 22 (55%)	111 ± 43 (100%)	17 ± 9 (16%)	18 ± 7 (16%)	5 ± 2 (5%)	9 ± 3 (8%)
2050s-2.6	58 ± 22 (54%)	109 ± 45 (100%)	19 ± 11 (17%)	18 ± 7 (16%)	5 ± 2 (5%)	9 ± 4 (8%)
2100s-2.6	59 ± 23 (52%)	114 ± 51 (100%)	22 ± 13 (19%)	18 ± 8 (16%)	5 ± 2 (5%)	9 ± 4 (8%)
2050s-8.5	55 ± 23 (53%)	105 ± 49 (100%)	19 ± 13 (18%)	17 ± 8 (16%)	5 ± 2 (5%)	8 ± 4 (8%)
2100s-8.5	59 ± 22 (49%)	121 ± 53 (100%)	26 ± 17 (22%)	19 ± 8 (16%)	6 ± 2 (5%)	10 ± 4 (8%)

We also examined the mean life-long metabolic amount of physiological processes of the live larvae particles (Table 3), which helped to elucidate the cause for the change in individual weight. The proportion of respiration to consumption (ingestion) increased with warming (14% in case 1960s, 16% in case 2010s, 19% in case 2100s-2.6, and 22% in case 2100s-8.5). Consequently, the proportion of biomass (individual weight) decreased in warming cases because SDA, egestion, and excretion remained a constant proportion of consumption. This result was consistent with the estimation by Kishi et al. (2009) who suggested that the energy loss because of respiration was higher under warming conditions.

However, the individual weight of squid did not necessarily decrease with warming even if the respiration rate increased, because consumption itself also changed with warming. The mean consumption roughly increased with warming (Table 3). For example, it increased by 3% in case 2100s-2.6 and 8% in Case 2100s-8.5 compared with that of case 2010s, and increased by 30% in case 2100s-2.6 and 37% in case 2100s-8.5 as compared with that of case 1960s. The increasing trend was clear in the autumn-spawning cohort (S-Fig.11b in Supplementary Material 3).

A detailed analysis on the experienced water temperature and prey density proposed an optimal growth temperature range (OGTR) of 10 °C and 15 °C for Japanese flying squid at the young stage (Supplementary Material 4). For the autumn-spawning cohort, even in the most severe warming conditions (case 2100s-8.5), the water temperature along the larvae migration route in the late life stage did not exceed 15 °C, i.e., it was within the OGTR (Fig.7d). Therefore, ocean warming benefited individual growth in the autumn-spawning cohort, whose individual weight also showed a slight increase with warming (S-Fig. 11a in Supplementary Material 3).

5 Conclusions

We simulated the migration and growth of Japanese flying squid from spawning to a young life stage (182 days) for cases 1960s, 2010s, and 2050s and 2100 s under warning scenarios RCP2.6 and RCP8.5. Although the amount of spawning particles showed a slight decrease with warming, the number of young squid in the JS will be higher in the next 100 years than in current situations. In the warming cases, the spawning grounds shifted northward, the spawning time of the autumn-spawning cohort was delayed, and the migration routes of squid shifted northward. This partly offset the negative influences of warming on squid. Along the migration routes, the maximum temperature increment was less than 2 °C under the warming conditions. The increase in water temperature increased the survival rate of the autumn-spawning cohort and led to a larger stock size of squid in the JS. The warming favored the individual growth of Japanese flying squid when the temperature experienced by squid was lower than the OGTR (10–15 °C), but limited the individual growth when the temperature was above the OGTR. In the next 100 years, the growth of the autumn-spawning cohort has a possibility to benefit from warming and the individual weight also increased slightly in our model.

It must be noted that our simulation has an essential assumption: we did not consider the change of parent squid numbers under global warming conditions, which may affect the egg number, i.e., the number of particles in our study. In addition, our analysis on model results is limited to the particles in the JS. Although it will be a major challenge for the future, the modeling of squid migration inside and outside the JS over its complete life cycle by considering the swimming behavior of adult squid is necessary for a better understating of the effects of global warming on the Japanese flying squid.

Acknowledgements We want to thank Prof. Michio J. Kishi who provided us the individual growth module of squid, Prof. Yasunori Sakurai for his advice on our simulations, and Prof. Naoki Hirose at Kyushu University who support the work of Dr. Katsumi Takayama.

Funding information This study was financially supported by the Environment Research and Technology Development Fund (S-13) of the Ministry of the Environment, Japan; by the Ministry of Education, Culture, Sports, Science and Technology (MEXT), Japan, to a project on Joint Usage/Research Center - Leading Academia in Marine and Environment Pollution Research (LaMer); and by the National Natural Science Foundation of China (41576010).

References

Barange M, Merino G, Blanchard JL, Scholtens J, Harle J, Allison EH et al (2014) Impacts of climate change on marine ecosystem production in societies dependent on fisheries. Nat Clim Chang 4(3):211

Blanchard JL, Jennings S, Holmes R, Harle J, Merino G, Allen JI et al (2012) Potential consequences of climate change for primary production and fish production in large marine ecosystems. Philos Trans R Soc B: Biol Sci 367(1605):2979–2989

Cheung WW (2018) The future of fishes and fisheries in the changing oceans: fishes and fisheries in the changing oceans. J Fish Biol 92:790–803

Fisheries Agency of Japan and Japan Fisheries Research and Education Agency (2018) Resource evaluation of Japanese common squid on Autumn group 2018. pp, 48 http://abchan.fra.go.jp/digests2018/details/201819.pdf (in Japanese)

Free CM, Thorson JT, Pinsky ML, Oken KL, Wiedenmann J, Jensen OP (2019) Impacts of historical warming on marine fisheries production. Science 363(6430):979–983

Hirose N, Takayama K, Moon JH, Watanabe T, Nishida Y (2013) Regional data assimilation system extended to East Asian marginal seas. Umi to Sora 89:43–51

Japan Meteorological Agency, (2018). Climate Change Monitoring Report 2017

Kang YS, Kim JY, Kim HG, Park JH (2002) Long-term changes in zooplankton and its relationship with squid, *Todarodes pacificus*, catch in Japan/East Sea. Fish Oceanogr 11(6):337–346

Kidokoro H (2003) Stock assessment and management method for the Japanese common squid in Japan. Suisankanri Danwakaiho 30:18–35

Kidokoro H, Goto T, Nagasawa T, Nishida H, Akamine T, Sakurai Y (2010) Impact of a climate regime shift on the migration of Japanese common squid (*Todarodes pacificus*) in the Sea of Japan. ICES J Mar Sci 67(7): 1314–1322

Kidokoro H, Shikata T, Kitagawa S (2014) Forecasting the stock size of the autumn cohort of Japanese common squid (*Todarodes pacificus*) based on the abundance of trawl-caught juveniles. Hidrobiológica 24(1)

Kim JJ, Stockhausen W, Kim S, Cho YK, Seo GH, Lee JS (2015) Understanding interannual variability in the distribution of, and transport processes affecting, the early life stages of *Todarodes pacificus* using behavioral-hydrodynamic modeling approaches. Prog Oceanogr 138:571–583

Kim H, Takayama K, Hirose N, Onitsuka G, Yoshida T, Yanagi T (2019) Biological modulation in the seasonal variation of dissolved oxygen concentration in the upper Japan Sea. J Oceanogr 75(3):257–271

Kishi MJ, Nakajima K, Fujii M, Hashioka T (2009) Environmental factors which affect growth of Japanese common squid, *Todarodes pacificus*, analyzed by a bioenergetics model coupled with a lower trophic ecosystem model. J Mar Syst 78(2):278–287

Kobayashi S, Ota Y, Harada Y, Ebita A, Moriya M, Onoda H et al (2015) The JRA-55 reanalysis: general specifications and basic characteristics. J Meteorol Soc Jpn Ser II 93(1):5–48

Lee H-J, Yoon J-H, Kawamura H, Kang H-W (2003) Comparison of RIAMOM and MOM in modeling the East Sea/Japan Sea circulation. Ocean Polar Res 25:287–302

Mao X, Guo X, Wang Y, Takayama K (2019) Influences of global warming on the larval survival and transport of snow crab (*Chionoecetes opilio*) in the sea of Japan. Sustainability 11(8):2198

Mizuta R, Arakawa O, Ose T, Kusunoki S, Endo H, Kitoh A (2014) Classification of CMIP5 future climate responses by the tropical sea surface temperature changes. Sola 10:167–171

Moore JK, Fu W, Primeau F, Britten GL, Lindsay K, Long M et al (2018) Sustained climate warming drives declining marine biological productivity. Science 359(6380):1139–1143

Moss RH, Edmonds JA, Hibbard KA, Manning MR, Rose SK, Van Vuuren DP et al (2010) The next generation of scenarios for climate change research and assessment. Nature 463(7282):747–756

Murata M (1989) Population assessment, management and fishery forecasting for the Japanese common squid *Todarodes pacificus*. In: Caddy JR (ed) Marine invertebrate fisheries: their assessment and management. John Wiley and Sons, New York, pp 613–636

Peters GP, Andrew RM, Boden T, Canadell JG, Ciais P, Quéré CL et al (2012) The challenge to keep global warming below 2°C. Nat Clim Chang 3(1):2–4

Pörtner HO, Knust R (2007) Climate change affects marine fishes through the oxygen limitation of thermal tolerance. Science 315(5808):95–97

Rosa AL, Yamamoto J, Sakurai Y (2011) Effects of environmental variability on the spawning areas, catch, and recruitment of the Japanese common squid, *Todarodes pacificus* (Cephalopoda: Ommastrephidae), from the 1970s to the 2000s. ICES J Mar Sci 68(6):1114–1121

Sakurai Y, Bower JR, Nakamura Y (1998) Effect of temperature on development and survival of *Todarodes pacificus* embryos and paralarvae. Oceanogr Lit Rev 3(45):556

Sakurai Y, Kiyofuji H, Saitoh S, Goto T, Hiyama Y (2000) Changes in inferred spawning areas of *Todarodes pacificus* (Cephalopoda: Ommastrephidae) due to changing environmental conditions. ICES J Mar Sci 57(1):24–30

van Vuuren DP, Edmonds J, Kainuma M, Riahi K, Thomson A, Hibbard K et al (2011) The representative concentration pathways: an overview. Clim Chang 109(1):5–31

Wakamatsu S, Oshio K, Ishihara K, Murai H, Nakashima T, Inoue T (2017) Estimating regional climate change uncertainty in Japan at the end of the 21st century with mixture distribution. Hydrol Res Lett 11(1):65–71

Watanabe K, Sakurai Y, Segawa S, Okutani T (1996) Development of the ommastrephid squid *Todarodes pacificus*, from fertilized egg to the rhynchoteuthion paralarva. Am Malacol Bull 13(1/2):73–88

Affiliations

Fei Ji[1,2] **· Xinyu Guo**[2] **· Yucheng Wang**[2,3] **· Katsumi Takayama**[4]

[1] Key Laboratory of Marine Environment and Ecology, Ocean University of China, Ministry of Education, 238 Songling Road, Qingdao 266100, China

[2] Center for Marine Environmental Studies, Ehime University, 2-5 Bunkyo-Cho, Matsuyama 790-8577, Japan

[3] Present address: Pilot National Laboratory for Marine Science and Technology, 1 Wenhai Road, Qingdao 266237, China

[4] Research Institute for Applied Mechanics, Kyushu University, Kasuga, Japan